Appl. Phys. B 86, 229–233 (2007)
DOI: 10.1007/s00340-006-2404-x

Applied Physics B
Lasers and Optics

L. LABATE[1,2,✉]
M. GALIMBERTI[1,3]
A. GIULIETTI[1,3]
D. GIULIETTI[1,3,4]
P. KÖSTER[1,3,4]
P. TOMASSINI[1,3]
L.A. GIZZI[1,3]

Study of forward accelerated fast electrons in ultrashort Ti K_α sources

[1] Intense Laser Irradiation Laboratory, IPCF, CNR, via Moruzzi 1, 56124 Pisa, Italy
[2] Laboratori Nazionali di Frascati, INFN, via E. Fermi 40, 00044 Frascati (Roma), Italy
[3] INFN, Sezione di Pisa, largo B. Pontecorvo 3, 56127 Pisa, Italy
[4] Dip. Fisica, Università di Pisa, largo B. Pontecorvo 3, 56127 Pisa, Italy

Received: 22 May 2006
Published online: 3 August 2006 •

ABSTRACT The results of an experiment aimed at studying hot electrons emerging from a target rear side in ultrashort laser-based K_α sources are described. In particular, forward accelerated fast electrons propagating through a Ti foil are found to be emitted in a cone perpendicular to the target surface. The energy of these electrons is estimated as well as their divergence. A comparison of the experimental findings with the results of a PIC simulation is also reported, aimed at identifying the physical processes responsible for the production of this forward propagating electron population.

PACS 52.38.-r; 52.38.kd; 52.38.Ph

1 Introduction

Laser-produced plasmas are currently recognized as one of the most promising ultrashort X-ray sources (see [1, 2] and references therein). Indeed, the development of powerful femtosecond laser systems based on the chirped pulse amplification technique [3] allowed a new interaction regime to be explored, characterized by high laser intensity and ultrashort pulse duration, which leads to the production of X-ray radiation in the keV energy range due to inner shell transitions in the cold target material [4]. In principle, X-ray pulses with a duration comparable to the laser pulse duration and source size comparable to the laser focal spot size can be achieved [5, 6].

As it is well known, the primary process for X-ray production from intense laser irradiation of solids is the generation of one or more populations of fast, or hot, electrons, having energies of the order of some tens to a few hundreds of keV [7–9]. Several mechanisms can be responsible for the generation of such electrons (see for example [10] and [11]). In particular, for the interaction parameters typical of the experimental regime considered in this paper, resonance absorption and vacuum heating are expected to be the dominant conversion processes of laser energy into hot electron kinetic energy [12–14]. In fact, in the case of p-polarized laser radiation, efficient energy transfer of laser energy to the plasma can occur through resonance absorption [15], giving rise to longitudinal electrostatic electron plasma waves. The subsequent damping of the plasma wave, occurring through collisionless processes, leads to the generation of a population of fast electrons. These energetic electrons can penetrate into the underlying cold target material, where they knock out electrons preferentially from the inner electronic shells of the atoms or ions [16, 17]. The radiative transitions of electrons from the outer shells finally leads to the generation of characteristic K lines. In the presence of very steep density gradients, the resonance absorption process is less effective and vacuum heating [18] can be responsible for the generation of hot electrons [19].

Since the main characteristics of K_α based ultrashort X-ray sources, such as photon yields as well as duration and size, strongly depend upon the production and transport processes of the fast electrons in matter, the understanding of this issue plays a crucial role when laser-plasma based K_α sources have to be modeled and their applications have to be considered (see [20] and references therein). In turn, K_α emission spectroscopy of neutral or partially ionized atoms, possibly with spatial resolution, can be exploited for studying the fast electron transport through matter with micrometer resolution [21, 22]. Furthermore, the transport properties of fast electrons play a major role in the fast ignition approach to the inertial confinement fusion [23, 24]. In view of these considerations, a major effort has been devoted in the last years to the study, both theoretical and experimental, of important physical issues, such as the return current and the influence of the self-generated electromagnetic fields on the electron transport [12, 25–27]. From the point of view of applications, this effort yielded important advances like the generation of monoenergetic fast electrons produced in ultrashort laser interaction with solids, as demonstrated by recent dedicated electron diffraction experiments [28, 29].

From an experimental viewpoint, an extensive study of the energy and angular distribution of the fast electrons has been carried out in the last few years. In particular, well defined angular peaks [30, 31], coming from different processes [32, 33], were identified in the investigation of fast electrons emerging from the front side of laser irradiated targets. Fast electrons propagating forward through the target are also currently studied [30, 34], to investigate the issues related to their transport through the solid. This has been done, in par-

✉ Fax: +39 050 315 2230, E-mail: luca@ipcf.cnr.it

ticular, by looking at the Bremsstrahlung emission of these electrons during the propagation through the target [31, 35].

In this paper we report on the direct observation of fast electrons on the rear side of a Ti thin foil irradiated by an ultrashort laser pulse at a moderate intensity ($a = p_e/m_e c \simeq 0.15$), typical of many high repetition rate laboratory K_α sources. The K_α emission from the target was also monitored. In the following section an overview of the experimental setup is given and the basic diagnostics for the detection of the fast electrons generated in the forward direction is described. The K_α emission diagnostics are also briefly introduced. The experimental results are then presented and discussed. A comparison with a PIC simulation is also made, followed by a discussion of the physical processes accounting for the forward electrons.

2 Experimental setup

A schematic view of the experimental setup is shown in Fig. 1. The laser pulse is generated by a Ti:Sa system delivering an energy up to 15 mJ on the target at a repetition rate of 10 Hz. The FWHM of the temporal profile of the pulse, measured by means of a second order auto-correlator, is about 65 fs. The pulse is focused using an $f/20$ lens onto the surface of a 12.5 μm thick Ti foil at an angle of incidence of about 40°. The target is moved horizontally or vertically to ensure a fresh interaction surface for each laser pulse in multi-shot measurements. The size of the focal spot was evaluated by means of an equivalent plane monitor technique to be of about 15 μm. The Rayleigh length is approximately 400 μm. Considering these values, the peak intensity on the target can be estimated to be $I_L \simeq 5 \times 10^{16}$ W/cm^2. We observe here that the relatively long Rayleigh length ensures that a plane wave is interacting with the target, even for small displacements from the focal spot, so that a well defined laser wavevector exists whose direction can be safely identified with respect to that of the detected electrons.

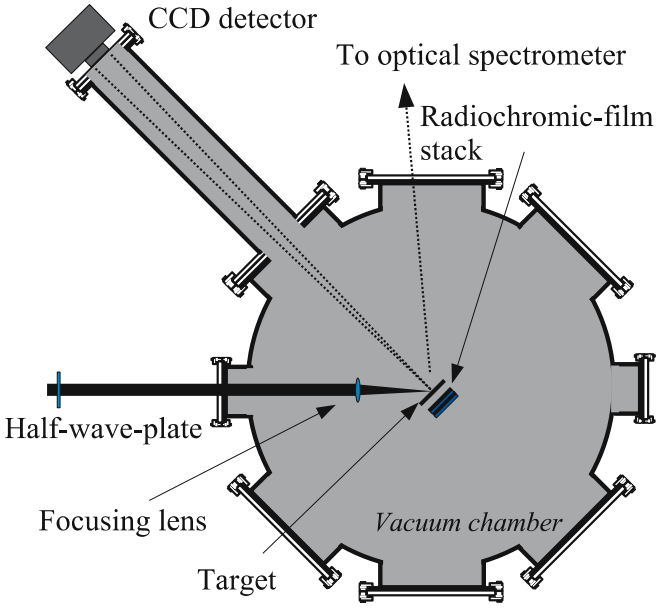

FIGURE 1 Schematic view of the experimental setup

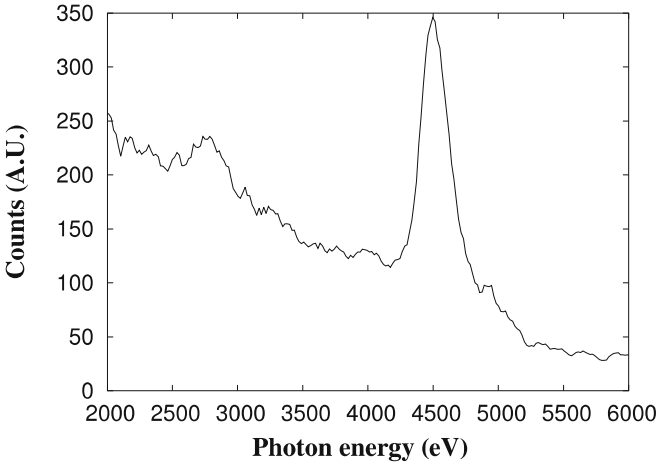

FIGURE 2 X-ray emission spectrum around the cold Ti K_α line. Adjacent to this line at 4.51 keV, the K_β line at 4.93 keV is also visible. The broad peak around 2.7 keV is due to K_α or K_β escape events

The fast electrons generated during the interaction, and passing through the Ti foil, were detected by means of a stack of radiochromic films placed behind the target, at a distance of about 5 mm from it. The energy and the angular distribution of the electrons could be retrieved by means of an original reconstruction algorithm [36] based upon a Montecarlo simulation employing the CERN library GEANT 4.2.0 [37]. In particular, two HD810 radiochromic layers were used in our case, packed in a 12.5 μm Al foil. We observe here that energetic particles leaving a detectable signal onto the radiochromic films were identified as electrons since the usage of proton sensitive CR39 films led to a null result.

The X-ray emission from the Ti target was also analyzed using a back-illuminated cooled CCD detector placed at about 1 meter from the source. This distance allowed the CCD detector to operate in the so-called single photon regime. As it is well-known, provided the detector response to different energy photons is known, this detection technique enables the spectral properties as well as the incident X-ray flux to be simultaneously measured [38]. Therefore, a reliable estimate of the X-ray photon yield without an independent calibration was possible in our experiment. Figure 2 shows a typical spectrum of the X-ray emission from our p-polarized laser irradiated target around the Ti K_α line at 4.51 keV. Taking into account the solid angle of view of the CCD detector and assuming an isotropic distribution of the emission, we estimated that approximately 10^7 K_α photons per pulse are emitted by our source.

3 Discussion of the experimental results

The first layer of a couple of radiochromic (rc) films, shown in Fig. 3, shows the signal obtained from a sequence of 100 p-polarized laser shots. A broad spot is visible in the lower part of the rc film image. According to the geometry of the experiment, the center of this spot corresponds to the direction of the target normal. Therefore, this spot is due to the presence of energetic electrons accelerated in this direction and passing through the target. The smaller, darker spot visible in the upper region, is a marker obtained by fir-

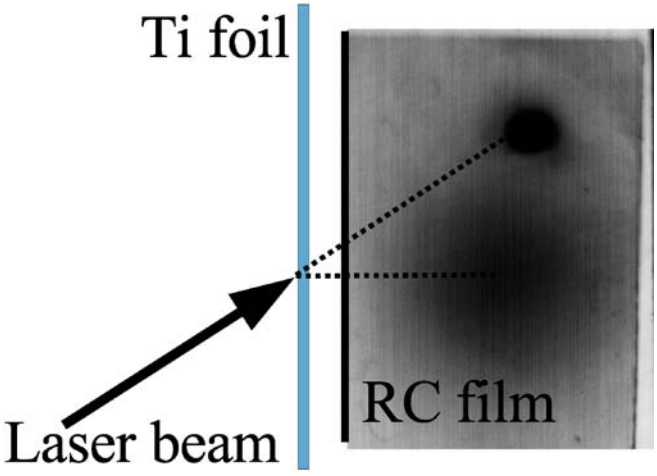

FIGURE 3 Image of the first (that is, nearest to the target) rc film obtained from a sequence of 100 p-polarized laser shots

ing a sequence of some shots while keeping the target in the same position (and thus producing a hole). This marker thus provides a reference for the direction of the laser beam, at around 40° with respect to the target normal. According to these considerations, we can conclude that in our experiment the electrons are emitted forward in the direction perpendicular to the target plane.

The energy of the electrons forming the broader spot can be estimated by means of Monte Carlo simulations accounting for the energy deposition in each of the rc film layers as stacked in our experimental conditions. Figure 4 shows the energy released by an electron in the first two rc layers as a function of its kinetic energy when leaving the rear side of the target. According to the plot and taking into account the detection threshold of the rc films, since no detectable signal was typically observed in the second layer, an energy of some tens up to hundreds of keV can be estimated for the electrons emitted forward and perpendicular to the target surface, which are responsible for the signal visible in Fig. 3.

As discussed above in Sect. 1, the production of a population of hot electrons is a basic issue in the interaction of

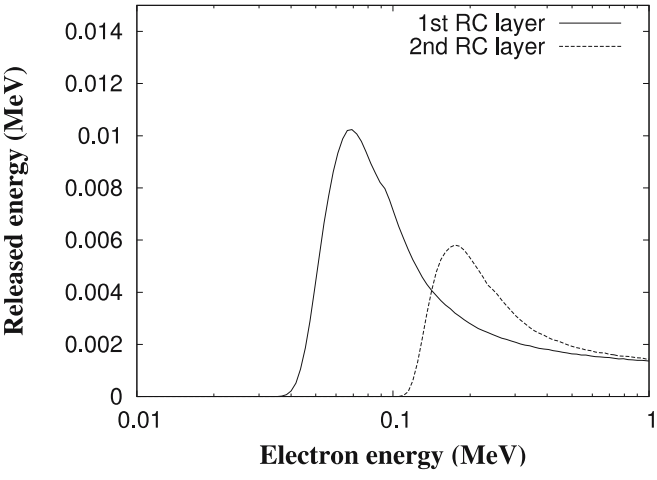

FIGURE 4 Energy released by an electron in each of the first two rc films in our experimental conditions as a function of the electron kinetic energy. Calculations are shown based on the Monte Carlo library GEANT 4.2.0 [37]

ultrashort laser pulses with solids. Depending on the dominant mechanism leading to the production of these electrons, different scaling laws have been proposed for the electron temperature as a function of the laser intensity, either on the basis of PIC simulations or based upon experimental data. In our experiment the hot electron temperature which can be deduced from the above considerations agrees quite well with the one proposed in [39]. In that work, the scaling law $T_{\text{hot}} \simeq 110(I_{17})^{1/2}$ keV, where I_{17} stands for the laser intensity in units of 10^{17} W/cm^2, has been given, based upon PIC simulations. In our case, this would give an electron temperature of about 77 keV. As we will see below, this was also our finding from PIC simulations for the temperature of the electrons having their momentum in a well-defined cone with respect to the target normal. A different scaling law has been suggested in [22], based upon experimental data. In our case, this law would give a lower electron temperature compared to the observed one.

Beside their temperature, the distribution of the initial propagation direction of the fast electrons is of a major concern when considering the size of the X-ray emission region in ultrashort laser-plasma K_α sources. This is a quite complex task, as it depends upon a number of parameters (see for example [40] and references therein).

An estimate of the angular spread of the electrons passing through the target can be retrieved, neglecting the space-charge effects of the electron bunch, by considering the size of the spot produced onto the rc film. By making simple geometrical considerations, the signal in Fig. 3 gives an aperture angle of 17° HWHM for the direction of the observed electrons.

In order to gain some insights into possible physical processes responsible for the observed features, 2D simulations were carried out by means of a PIC (particles-in-cell) code. The initial density map was set according to the results of hydrodynamics simulations performed using the code POLLUX [41]. In fact, the hydro-code was used to predict the properties of the pre-plasma generated by the pedestal (due to the amplified spontaneous emission) of the main pulse and low level prepulses. According to these simulations, the density scalelength at the critical density layer is expected to be of the order of the laser wavelength. PIC simulations carried out using this value of the scalelength at the critical density show that most of the fast electrons are generated in a thin layer around the critical surface. Since we are interested here in the electrons detected at the rear side of the target, we report in Fig. 5 the energy distribution, as gained by the PIC simulations, of the electrons having the direction of their momentum in a cone of semi-aperture of 17° with respect to the normal to the target surface. The distribution was fitted using the sum of two Maxwellian functions, whose resulting temperatures were about 13 and 83 keV. The presence of two different temperatures for the hot electrons is already known and can be attributed to different generation processes [19, 42]. According to this fit, a temperature of about 83 keV is expected for our rear side electrons. As already anticipated above, this value of temperature agrees with theoretical and numerical models given in the literature (see for example [19, 42, 43]). This agreement implies that a major role is played in our experimental conditions by either the resonance absorption or

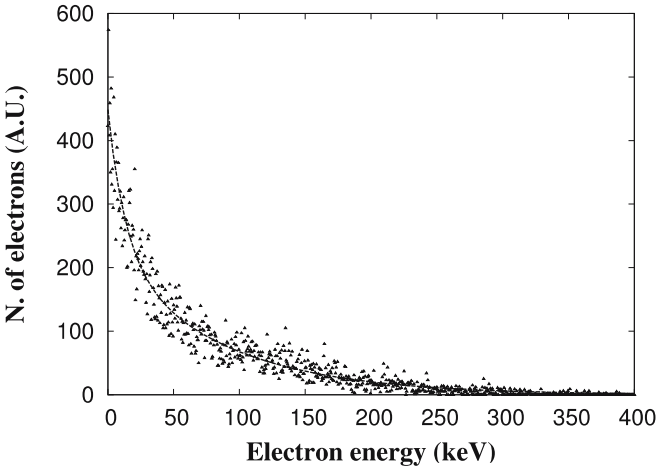

FIGURE 5 Energy distribution of the electrons having their momentum oriented in a cone of semi-aperture of 17° with respect to the inward normal to the target surface, as retrieved by a PIC simulation. The *curve* resulting from a fit with the sum of two Maxwellian functions is also shown

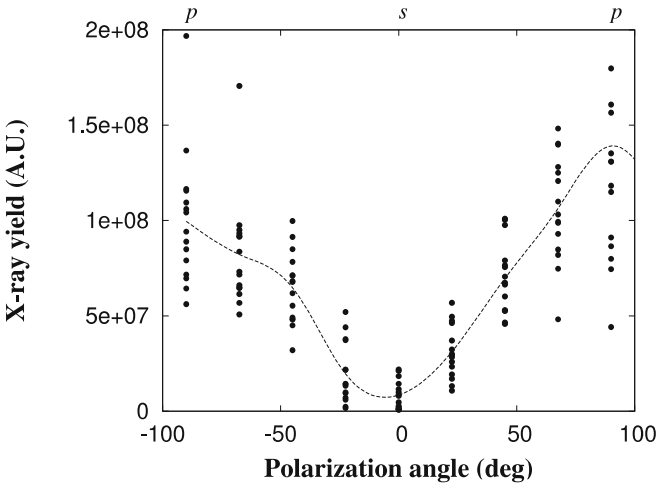

FIGURE 6 X-ray emission yield as a function of the polarization angle of the laser beam. The angle $\vartheta = 0°$ corresponds to an *s*-polarized beam and the angles $\vartheta = \pm 90°$ correspond to a *p*-polarized beam

the vacuum heating processes. In these circumstances, we also expect that the process is sensitive to the polarization of the laser pulse. In fact, although the rippling of the critical surface due to target surface imperfections can account for the production of hot electrons in the plasma even in the case of *s*-polarized laser beams [10], K_α emission yields strongly depend upon the laser polarization. In addition, the small aperture of our focusing optics and the long Rayleigh length used in our experiment are expected to enhance the difference between *s* and *p* polarizations. A study of the K_α emission yield as a function of the laser polarization was carried out by inserting a rotating half-wave plate in the beam path before the focusing lens. The laser system is *p*-polarized at the exit of the laser system. By rotating the half-wave plate, the polarization of the laser radiation can be changed continuously from *p* to *s*. In our experiment, the polarization was changed stepwise from *p* to *s* and again to *p*. For each polarization configuration, the signal from the CCD detector was considered as a measure of the K_α emission signal. Figure 6 shows this signal as a function of the rotation angle of the half-wave plate. A strong dependence of the X-ray signal on the polarization of the laser light is clearly visible, being more than one order of magnitude higher for *p*-polarized laser light than for the *s*-polarized light. This result indicates that the process playing the dominant role in our experimental configuration is sensitive to the polarization of the laser light, as expected in the case of resonance absorption or vacuum heating. A possible way to discriminate between these two effects is to take into account the fact that a typical signature of resonance absorption in these experiments is the generation of second harmonic emission in the direction of specular reflection, as previously observed [14]. Although a conclusive study of optical scattering is still in progress, preliminary observations indicate that no detectable second harmonic emission is found in the conditions discussed here. Also, the value of the scalelength at the critical density predicted by the hydrocode could be significantly lower than the conservative value used here. Both of these considerations would make vacuum heating the preferred mechanism to explain the observed features.

4 Summary and conclusions

The observation of a population of forward accelerated electrons through Ti foils irradiated at an intensity of about 5×10^{16} W/cm^2 has been reported. The electrons were observed at the rear side of a 12.5 μm thick target by means of an rc film stack detector. The electron energy and their angular spread was estimated. The temperature of the observed electrons fits well with previously suggested scaling laws based on the assumption that the main process responsible for their production, in conditions similar to the ones of this experiment, is resonance absorption or vacuum heating. This was confirmed in our work by the K_α emission yield dependence on the laser polarization showing a strong dependence on the polarisation and with a much higher yield for *p*-polarized laser light. PIC simulations carried out on our interaction regime show that the temperature of the electrons having the same propagation direction as the ones observed at the rear side of the target is in quite a good agreement with the one estimated experimentally. The propagation direction of the electrons was found to be perpendicular to the target surface, i.e. parallel to the expected plasma density gradient, which also confirms that the main responsible processes for their production are either the resonance absorption or the vacuum heating. Additional considerations based upon optical scattering and laser contrast indicate that vacuum heating may be the most likely to occur. This study can be useful for the investigation and the optimization of ultrashort laser-based K_α sources, in particular for those issues related to the hot electrons transport through the solid target.

ACKNOWLEDGEMENTS We would like to thank A. Barbini, W. Baldeschi and M. Voliani for technical assistance. This work was supported by the MIUR project 'Impianti innovativi multiscopo per la produzione di radiazione X e ultravioletta'. L.L and P.T acknowledge financial support from the INFN project PLASMONX.

REFERENCES

1 A. Rousse, C. Rischel, J.-C. Gauthier, Rev. Mod. Phys. **73**, 17 (2001)
2 D. Giulietti, L.A. Gizzi, La Rivista del Nuovo Cimento **21**, 1 (1998)
3 D. Strickland, G. Mourou, Opt. Commun. **56**, 219 (1985)

4 A. Rousse, P. Audebert, J.P. Geindre, F. Falliès, J.C. Gauthier, A. Mysyrowicz, G. Grillon, A. Antonetti, Phys. Rev. E **50**, 2200 (1994)
5 C. Reich, I. Uschmann, F. Ewald, S. Düsterer, A. Lübcke, H. Schwoerer, R. Sauerbrey, E. Förster, Phys. Rev. E **68**, 056408 (2003)
6 T. Feurer, A. Morak, I. Uschmann, C. Ziener, H. Schwoerer, C. Reich, P. Gibbon, E. Förster, R. Sauerbrey, Phys. Rev. E **65**, 016412 (2001)
7 T. Schlegel, S. Bastiani, L. Grémillet, J.-P. Geindre, P. Audebert, J.-C. Gauthier, E. Lefebvre, G. Bonnaud, J. Delettrez, Phys. Rev. E **60**, 2209 (1999)
8 K.B. Wharton, S.P. Hatchett, S.C. Wilks, M.H. Key, J.D. Moody, V. Yanovsky, A. Offenberger, B.A. Hammel, M.D. Perry, C. Joshi, Phys. Rev. Lett. **81**, 822 (1998)
9 D. Salzmann, C. Reich, I. Uschmann, E. Förster, P. Gibbon, Phys. Rev. E **65**, 036402 (2002)
10 S.C. Wilks, W.L. Kruer, IEEE J. Quantum Electron. **QE-33**, 1954 (1997)
11 G. Malka, M.M. Aleonard, J.F. Chemin, G. Claverie, M.R. Hartson, J.N. Scheurer, V. Tikhonchuk, S. Fritzler, V. Malka, P. Balcou, G. Grillon, Phys. Rev. E **66**, 066402 (2002)
12 J. Zhang, Y.T. Li, Z.M. Sheng, Z.Y. Wei, X. Dong, Q.L. Lu, Appl. Phys. B **80**, 957 (2005)
13 P. Gibbon, E. Förster, Plasma Phys. Contr. F. **38**, 769 (1996)
14 L.A. Gizzi, A. Giulietti, D. Giulietti, P. Audebert, S. Bastiani, J.-P. Geindre, A. Mysyrowicz, Phys. Rev. Lett. **76**, 2278 (1996)
15 D. Riley, J.J. Angulo-Gareta, F.J. Khattak, M.J. Lamb, P.S. Foster, E.J. Divall, C.J. Hooker, A.J. Langley, R.J. Clarke, D. Neely, Phys. Rev. E **71**, 016406 (2005)
16 F. Ewald, H. Schwoerer, R. Sauerbrey, Europhys. Lett. **60**, 710 (2002)
17 S.B. Hansen, A.Y. Faenov, T.A. Pikuz, K.B. Fournier, R. Shepherd, H. Chen, K. Widmann, S.C. Wilks, Y. Ping, H.K. Chung, A. Niles, J.R. Hunter, G. Dyer, T. Ditmire, Phys. Rev. E **72**, 036408 (2005)
18 F. Brunel, Phys. Rev. Lett. **59**, 52 (1987)
19 P. Gibbon, A.R. Bell, Phys. Rev. Lett. **68**, 1535 (1992)
20 J.R. Davies, Phys. Rev. E **65**, 026407 (2002)
21 R. Freeman, C. Anderson, J.M. Hill, J. King, R. Snavely, S. Hatchett, M. Key, J. Koch, A. MacKinnon, R. Stephens, T. Cowan, J. Quantum Spectrosc. Radiat. Transf. **81**, 183 (2003)
22 H. Nishimura, T. Kawamura, R. Matsui, Y. Ochi, S. Okihara, S. Sakabe, F. Koike, T. Johzaki, H. Nagatomo, K. Mima, I. Uschmann, E. Förster, J. Quantum Spectrosc. Radiat. Transf. **81**, 327 (2003)
23 A. Macchi, A. Antonicci, S. Atzeni, D. Batani, F. Califano, F. Cornolti, J.J. Honrubia, T.V. Lisseikina, F. Pegoraro, M. Temporal, Nucl. Fusion **43**, 362 (2003)
24 M.H. Key, M.D. Cable, T.E. Cowan, K.G. Estabrook, B.A. Hammel, S.P. Hatchett, E.A. Henry, D.E. Hinkel, J.D. Kilkenny, J.A. Koch, W.L. Kruer, B. Langdon, B.F. Lasinski, R.W. Lee, B.J. MacGowan, A. MacKinnon, J.D. Moody, M.J. Moran, A.A. Offenberger, D.M. Pennington, M.D. Perry, T.J. Phillips, T.C. Sangster, M.S. Singh, M.A. Stoyer, M. Tabak, G.L. Tietbohl, M. Tsukamoto, K. Wharton, S.C. Wilks, Phys. Plasmas **5**, 1966 (1998)
25 A.R. Bell, J.R. Davies, S. Guerin, H. Ruhl, Plasma Phys. Contr. F. **39**, 653 (1997)
26 D. Batani, J.R. Davies, A. Bernardinello, F. Pisani, M. Koenig, T.A. Hall, S. Ellwi, P. Norreys, S. Rose, A. Djaoui, D. Neely, Phys. Rev. E **61**, 5725 (2000)
27 F. Pisani, A. Bernardinello, D. Batani, A. Antonicci, E. Martinolli, M. Koenig, L. Gremillet, F. Amiranoff, S. Baton, J. Davies, T. Hall, D. Scott, P. Norreys, A. Djaoui, C. Rousseaux, P. Fews, H. Bandulet, H. Pepin, Phys. Rev. E, **62**, R5927 (2000)
28 R. Tommasini, E.E. Fill, R. Bruch, G. Pretzler, Appl. Phys. B **79**, 923 (2004)
29 E.E. Fill, S. Trushin, R. Bruch, R. Tommasini, Appl. Phys. B **81**, 155 (2005)
30 Z. Li, H. Daido, A. Fukumi, A. Sagisaka, K. Ogura, M. Nishiuchi, S. Orimo, Y. Hayashi, M. Mori, M. Kado, S.V. Bulanov, T.Zh. Esirkepov, Y. Oishi, T. Nayuki, T. Fujii, K. Nemoto, S. Nakamura, A. Noda, Phys. Plasmas **13**, 043104 (2006)
31 L.M. Chen, J. Zhang, Y.T. Li, H. Teng, T.J. Liang, S.M. Sheng, Q.L. Dong, L.Z. Zhao, Z.Y. Wei, X.W. Tang, Phys. Rev. Lett. **87**, 225001 (2001)
32 Y. Sentoku, H. Ruhl, K. Mima, R. Kodama, K.A. Tanaka, Y. Kishimoto, Phys. Plasmas **6**, 2855 (1999)
33 H. Ruhl, Y. Sentoku, K. Mima, K.A. Tanaka, R. Kodama, Phys. Rev. Lett. **82**, 743 (1999)
34 V.S. Rastunkov, V.P. Krainov, Phys. Plasmas **13**, 023104 (2006)
35 P.A. Norreys, M. Santala, E. Clark, M. Zepf, F. Watts, F.N. Beg, K. Krushelnick, M. Tatarakis, A.E. Dangor, X. Fang, P. Graham, T. McCanny, R.P. Singhal, K.W.D. Ledingham, A. Creswell, D.C.W. Sanderson, J. Magill, A. Machacek, J. Wark, R. Allott, B. Kennedy, D. Neely, Phys. Plasmas **6**, 2150 (1999)
36 M. Galimberti, A. Giulietti, D. Giulietti, L.A. Gizzi, Rev. Sci. Instrum. **76**, 053303 (2005)
37 S. Agostinelli, J. Allison, K. Amako, J. Apostolakis, H. Araujo, P. Arce, M. Asai, D. Axen, S. Banerjee, G. Barrand, F. Behner, L. Bellagamba, J. Boudreau, L. Broglia, A. Brunengo, H. Burkhardt, S. Chauvie, J. Chuma, R. Chytracek, G. Cooperman, G. Cosmo, P. Degtyarenko, A. Dell'Acqua, G. Depaola, D. Dietrich, R. Enami, A. Feliciello, C. Ferguson, H. Fesefeldt, G. Folger, F. Foppiano, A. Forti, S. Garelli, S. Giani, R. Giannitrapani, D. Gibin, J.J. Gómez Cadenas, I. González, G. Gracia Abril, G. Greeniaus, W. Greiner, V. Grichine, A. Grossheim, S. Guatelli, P. Gumplinger, R. Hamatsu, K. Hashimoto, H. Hasui, A. Heikkinen, A. Howard, V. Ivanchenko, A. Johnson, F.W. Jones, J. Kallenbach, N. Kanaya, M. Kawabata, Y. Kawabata, M. Kawaguti, S. Kelner, P. Kent, A. Kimura, T. Kodama, R. Kokoulin, M. Kossov, H. Kurashige, E. Lamanna, T. Lampén, V. Lara, V. Lefebure, F. Lei, M. Liendl, W. Lockman, F. Longo, S. Magni, M. Maire, E. Medernach, K. Minamimoto, P. Mora de Freitas, Y. Morita, K. Murakami, M. Nagamatu, R. Nartallo, P. Nieminen, T. Nishimira, K. Ohtsubo, M. Okamura, S. O'Neale, Y. Oohata, K. Paech, J. Perl, A. Pfeiffer, M.G. Pia, F. Ranjard, A. Rybin, S. Sadilov, E. Di Salvo, G. Santin, T. Sasaki, N. Savvas, Y. Sawada, S. Scherer, S. Sei, V. Sirotenko, D. Smith, N. Starkov, H. Stoecker, J. Sulkimo, M. Takahata, S. Tanaka, E. Tcherniaev, E. Safai Tehrani, M. Tropeano, P. Truscott, H. Uno, L. Urban, P. Urban, M. Verderi, A. Walkden, W. Wander, H. Weber, J.P. Wellish, T. Wenaus, D.C. Williams, D. Wright, T. Yamada, H. Yoshida, D. Zschiesche, Nucl. Instrum. Methods Phys. Res. A **506**, 250 (2003)
38 L. Labate, M. Galimberti, A. Giulietti, D. Giulietti, L.A. Gizzi, P. Tomassini, G. Di Cocco, Nucl. Instrum. Methods Phys. Res. A **495**, 148 (2002)
39 C. Reich, P. Gibbon, I. Uschmann, E. Förster, Phys. Rev. Lett. **84**, 4846 (2000)
40 J. Zhang, J. Zhang, Z.M. Sheng, Y.T. Li, Y. Qiu, Z Jin, H. Teng, Phys. Rev. E **69**, 046408 (2004)
41 G.J. Pert, J. Comput. Phys. **43**, 111 (1981)
42 L.M. Chen, J. Zhang, Q.L. Dong, H. Teng, T.J. Liang, L.Z. Zhao, Z.Y. Wei, Phys. Plasmas **8**, 2925 (2001)
43 Q.L. Dong, J. Zhang, H. Teng, Phys. Rev. E **64**, 026411 (2001)